CONF-9011168--1

ACCELERATING AND STORING POLARIZED HADRON BEAMS*

L. C. Teng

Argonne National Laboratory, Argonne, Illinois, U.S.A.

CONF-9011168--1

DE91 006464

October, 1990

Introduction

Polarization hadron experiments at high energies continue to generate surprises. Many questions remain unanswered or unanswerable within the frame work of QCD. These include such basic questions as to why at high energies the polarization analyzing power in pp elastic scattering remains high, why hyperons are produced with high polarizations etc. It is, therefore, interesting to investigate the possibilities of accelerating and storing polarized beams in high energy colliders.

On the technical side the recent understanding and confirmation of the actions of partial and multiple Siberian snakes made it possible to contemplate accelerating and storing polarized hadron beams to multi-TeV energies.

In this paper, we will examine the equipment, the operation and the procedure required to obtain colliding beams of polarized protons at TeV energies.

*Work supported by the U.S. Department of Energy, Advanced Photon Source under Contract W-31-109-Eng-38.

Polarized H^- Source

Beam stacking with charge-exchange injection into a circular accelerator offers the most promising procedure for acquiring a high intensity polarized proton beam. For this we need the polarized H^- source. A polarized H^- source consists of two main sections. The first section produces a polarized H^0 beam. Many different schemes have been proposed and employed for this purpose. The most straightforward and traditional is the method of using the Stern-Gerlach mechanism to produce a neutral atomic hydrogen beam with electron spins polarized. The nucleus proton is then polarized through microwave transitions between hyperfine states in a magnetic field. In the second section, the H^0 is transformed to H^- through electron pickup from Cs atoms. Figs. 1 and 2 give schematic drawings of the two sections of such a source used for the AGS polarized beam.[1]

The highest currents obtained in operating H^- sources are so far no more than 30-50 μA. However sources capable of tens of mA are being developed and look promising.[2]

Acceleration Through Linacs

By now, the linac stage of the injector system is fairly well standardized. It generally starts with a 2-MeV, 400-MHz radio-frequency quadrupole (RFQ) linac

followed by sections of drift-tube linac (DTL) operating at the same frequency and accelerating the H^- ions to somewhat beyond 100 MeV. The beam is, then, further accelerated to 600-1000 MeV for injection into a synchrotron. This high energy linac structure consists of coupled cavity or disk-and-washer cells and operates at twice or three times the RFQ/DTL frequency.

In all these linac sections the transverse focusing of the beam is supplied by alternating-gradient electromagnetic elements producing electric and/or magnetic quadrupole fields. Although the spin is affected dynamically by these focusing elements the alternating nature causes their effects to cancel in successive elements. Thus, the polarization is preserved throughout the linac sections.

Depolarizing Resonance in Synchrotrons

In a synchrotron the spin precesses about the guide magnetic field. The spin precession over a full revolution may be considered as a single precession of angle $2\pi\nu_s$ about some "eigenspin" direction. If the spin tune, ν_s, runs onto some rational relationship with the revolution, the sector or the orbital oscillation periodicity (resonance condition) the undesirable precession can accumulate to a sizeable depolarization. These spin resonances must be avoided or eliminated.

More specifically, in an ideal horizontal planar synchrotron the eigenspin direction is vertical and the spin tune is $\nu_s = \gamma G$ where γ is the relativistic energy and

$$G = \frac{g-2}{2} = 1.793$$

is the anomalous gyromagnetic ratio of the proton. In a real machine there are two sources of horizontal field components producing depolarizing horizontal precessions. First, construction errors lead to distortions in the closed orbit away from a perfectly horizontal plane. The horizontal field component causing the vertical distortion is proportional to the magnitude of the distortion and has the revolution periodicity, i.e. harmonics k (=integer). Second, for particles performing vertical oscillation there is an additional horizontal field component. This field is proportional to the amplitude of the oscillation and has harmonics $kP \pm \nu_z$ where P is the lattice sector periodicity and ν_z is the vertical oscillation tune. The resonance conditions are therefore

$$\nu_s = \gamma G = \begin{cases} k & \text{imperfection resonance} \\ kP \pm \nu_z & \text{intrinsic resonance} \end{cases} \qquad (1)$$

As the proton is accelerated its spin tune crosses a large number of resonances in succession.

The width ϵ of a resonance expressed in spin tune units gives a measure of the strength of the resonance. It depends, in addition to the amplitude of

oscillation or orbit distortion, on the specific magnet lattice of the ring. Computer programs have been written to compute the resonance widths or to track spin precessions around any given machine. The amount of depolarization suffered in crossing a resonance is proportional to the width and inversely to the crossing speed. To reduce the depolarization effect, one must therefore either reduce the width or increase the crossing speed. Both methods have been applied in practice.[1] The width ϵ increases with energy for both types of resonance such that at high energies

$$\epsilon \propto \begin{cases} \gamma & \text{imperfection resonance} \\ \gamma^{1/2} & \text{intrinsic resonance} \end{cases} \qquad (2)$$

For imperfection resonances the orbit distortion is fixed and the horizontal field component is roughly proportional to γ. For intrinsic resonances the proportionality is softened because the amplitude of oscillation decreases as $\gamma^{-1/2}$. Thus for high energy machines, the stronger and more numerous resonances make the individual resonance jump and orbit correction method used so far, extremely unattractive. This is especially true since resonance jumping becomes totally inapplicable when resonances overlap. Fortunately, Derbenev and Kondratenko[3] proposed in 1977 an ingenious method of eliminating the resonances altogether using strings of dipoles to impart the equivalent of phase shifts to the vertical precession. The string of dipoles has come to be called the Siberian snake.

Siberian Snakes

If while an oscillation is being driven by a resonant force, its phase is periodically shifted by 180^{o} the force will then periodically excite and damp the oscillation amplitude, leading to no net blow-up, and the resonance is effectively eliminated. In practice, any sequence of small phase shifts which add up to more than 180^{o} before the oscillation amplitude becomes excessive will produce the same result. For spin resonances in a synchrotron the equivalent "phase" of the vertical precession can be shifted by a precession about a horizontal axis. The Siberian snake is a series of modest dipoles (~10 in number and ~1 Tm each) installed in a straight section of the synchrotron ring lattice, which produce a horizontal precession while causing no net deflection of the orbit. A general snake designated by (δ,α) produces a precession angle δ about an axis lying in the horizontal plane and at angle α from the transverse direction. We refer to δ as the strength and α as the axis angle of the snake. In this notation the standard full strength Type 1 (longitudinal precession axis) and Type 2 (transverse precession axis) snakes are denoted as $(\pi,\pi/2)$ and $(\pi,0)$ and are shown in Figs. 3 and 4. The variable precession snakes of Type 1, $(\delta,\pi/2)$, and Type 2, $(\delta,0)$, have been designed by D. Underwood.[4] These snakes and their tuning curves are shown in Figs. 5 to 8. Other partial snake configurations have also been investigated[5,6].

A solenoid acts like a Type 1 snake. However, for a longitudinal field to produce a given precession, the field strength must be proportional to γ which makes it impractical at high energies. Moreover, although a solenoid causes no orbit deflection, its focusing and horizontal/vertical coupling actions must be compensated by added skew quadrupoles.

Spin dynamics when expressed in the spinor formulation[7] can be studied in a manner analogous to the orbit dynamics in the matrix formulation. The one-revolution spinor transformation matrix gives the spin tune and the eigenspin direction, namely the orientation of the spin which returns after one full revolution. As stated earlier, without the snake the eigenspin direction is vertical and the spin tune is $\nu_s = \gamma G$. With a (δ,α) snake installed, spin tune is given by[8]

$$\cos \pi\nu_s = \cos \frac{\delta}{2} \cos \pi\gamma G \qquad (3)$$

Fig. 9 plots ν_s as a function of γG. The available value of ν_s is broken up into bands and the integer values are excluded. This comes about in much the same manner as the formation of the electron energy band structure in a solid. To avoid imperfection (integer) resonances the spin-tune gap must be larger than the resonance width.

Although the snakes produce no net distortion in the particle orbit external to the snakes, they unavoidably cause transverse orbit excursions inside. Since the transverse precessions, hence the strengths of the dipoles are independent of

particle energy, the excursions are larger at lower energies. The maximum excursions for each type of snake are given as functions of energy in the formulas supplementing Figs 3, 4, 5 and 7. On the other hand, the resonance widths are smaller at lower energies requiring only weaker snakes thereby keeping the orbit excursions within tolerable limits. As an example, for the low-energy booster (LEB) of the SSC, if one uses an Underwood Type 2 snake running at full strength at the final energy of 11 GeV the maximum orbit excursion is 7.3 cm and the maximum resonance width that can be suppressed is 0.5. If the orbit excursion is kept the same at all energies, at injection (600 MeV) one has (maximum width) = $\delta/2\pi$ = 0.0053. This range of maximum width is ample to handle all the resonances. The constant excursion mode of operation allows aligning the snake dipoles on the deformed orbit so that their apertures do not have to be enlarged to accommodate the orbit excursions.

Multiple Snakes at High Energies

Eq. (3) gives for the maximum resonance width of an isolated resonance that can be suppressed by a full-strength snake as

$$\epsilon_{max} = \begin{cases} 1/2 & \text{imperfection res.} \\ |1/2 - (\text{fractional part of } \nu_z)| & \text{intrinsic res.} \end{cases} \qquad (4)$$

For wider resonances one needs more than one full strength snakes. In what follows we will consider only full strength snakes with $\delta=\pi$. Generally one prefers an even number N of snakes because then the eigenspin directions are vertical, alternately up and down between snakes. The spin tune is then[9]

$$\nu_s = \frac{1}{2\pi} \sum_{i=1}^{N} (-)^i (2\alpha_i + \gamma G\theta_i) \tag{5}$$

where α_i is the axis angle of the ith snake and θ_i is the orbit turning angle from the ith snake to the (i+1)th snake. To make ν_s independent of energy the azimuthal locations of the snakes must be chosen such that

$$\sum_i (-)^i \theta_i = 0 \tag{6}$$

the spin tune is then

$$\nu_s = \frac{1}{\pi} \sum_i (-)^i \alpha_i \tag{7}$$

and should be adjusted to (integer + 1/2). The maximum width of a single isolated intrinsic resonance that can be suppressed by N snakes arranged in this manner is given by[9]

$$\sin \pi\frac{\epsilon_{max}}{N} = |\cos \pi\nu_z|^{1/2} \tag{8}$$

since ν_z is generally about 1/4 unit away from an integer this gives $\epsilon_{max} \approx 0.3N$. This result, simple as it is, is however not very useful in practice, because for these large widths one must deal with overlapping resonances. The closest, hence the

strongest overlapping resonances consist of a broad intrinsic resonance and its neighboring imperfection resonances. The dynamics of overlapping resonances is difficult to study analytically. The results of tracking studies by Lee and Courant[10] show that to effectively suppress such overlapping resonances the number of snakes required must satisfy:

$$\begin{cases} \epsilon(\text{intrinsic}) < 0.4\,\frac{N}{2} \\ \epsilon(\text{imperfection}) < 0.3\,\frac{N}{2} \end{cases} \qquad (9)$$

For SSC the strongest intrinsic resonance at 20 TeV has width ϵ(intrinsic)~5 and after careful orbit correction, the strongest imperfection resonance has ϵ(imperfection) ~ 0.6. Eq. 9 then gives for the minimum number of snakes

$$N \gtrsim 26 \qquad (10)$$

Experimental Studies of Siberian Snakes at IUCF

Although Siberian snakes were proposed in 1977 no experimental confirmation of their expected actions was made until 1988. This is mainly because of the shortage of available polarized beams. The layout of the Indiana University Cyclotron Facility (IUCF)[11] is shown in Fig. 10. The experimental set up for testing the Siberian snake in the IUCF Cooler Ring is shown diagrammatically in Fig. 11. The Type 1 snake is a superconducting solenoid and the Cooler Solenoids of the electron cooling system are used also to generate "error" horizontal field for adjusting the width of the imperfection resonance.

The depolarizing effects[12] of the $\nu_s = \gamma G = 2$ imperfection resonance at 108 MeV induced by the cooler solenoids are shown in Figure 12. Plotted are the vertical and horizontal polarizations of the beam at 120 MeV as functions of the strength, $\int B d\ell$, of the main cooler solenoid which is proportional to the width of the resonance. The effect of the Siberian snake in suppressing the resonance is clearly demonstrated in the Snake ON and Snake OFF data at 104 MeV given in Fig. 13. With a single Type 1 snake the eigenspin direction for Snake OFF is vertical and for Snake ON is radial. The polarization of the injected beam is adjusted accordingly.

The intrinsic resonance $\nu_s = \gamma G = -3+\nu_z$ at 177 MeV was studied[13] first by ramping ν_z through the resonance with the ring quadrupoles. The depolarization with the snake off is $[P/P_{inj}]_{vert} \approx 26\%$ and with the snake on is $[P/P_{inj}]_{rad} \approx 95\%$. The beam polarizations are plotted against ν_z in Fig. 14. This demonstrates clearly also the capability of the snake to suppress the intrinsic resonance. This experiment also exhibited the synchrotron oscillation satellite resonances

$$\nu_s = -3 + \nu_z \pm \nu_{syn} \qquad (11)$$

where ν_{syn} is the synchrotron oscillation tune, and showed that they are also suppressed by the snake.

Conclusions

The experiments on the IUCF prove conclusively that the computed actions of Siberian snake are quantitatively correct.

Together with earlier discussions we conclude that all depolarizing spin resonances in high energy colliders and their injector synchrotrons can be effectively suppressed by the use of partial and multiple Siberian snakes. For the SSC the total number of snakes needed and their parameters are reasonable. However, space must be provided for installation of the snakes.

References

1. F.Z. Khiari et al, Phys. Rev. D, 39, 45, (1989)
2. J.G. Alessi, Proc. 1987 IEEE Part. Accel. Conf. (Washington D.C. March, 1987) Vol 1, P. 249
3. Ya S. Derbenev and A.M. Kondratenko, Proc. 10th Int. Conf. on High Energy Accel., Protvino Vol. 2, p. 70 (1977)
4. D. G. Underwood, Argonne National Laboratory Report ANL-HEP-PR-88-71 (Nov. 1988)
5. K. Steffen, Particle Accelerators, 24, 45 (1989)
6. S.Y. Lee, Brookhaven National Laboratory Report, BNL-52248 (June, 1990)
7. B.W. Montague, Particle Accelerators, 11, 219 (1981)
8. T. Roser, AIP Conf. Proc. No. 187, Vol 2, p. 1442 (1989)
9. K. Steffen, AIP Conf. Proc. No. 145 p. 154 (1986)
10. S.Y. Lee and E.D. Courant, Phys. Rev. D 41, 292 (1990)
11. R.E. Pollock, IEEE Trans. on Nucl. Sci. NS-30, 2056 (1983)
12. A.D. Krisch et al, Phys. Rev. Lett. 63, 1137 (1989)
13. J.E. Goodwin et al, Phys. Rev. Lett. 64, 2779 (1990)

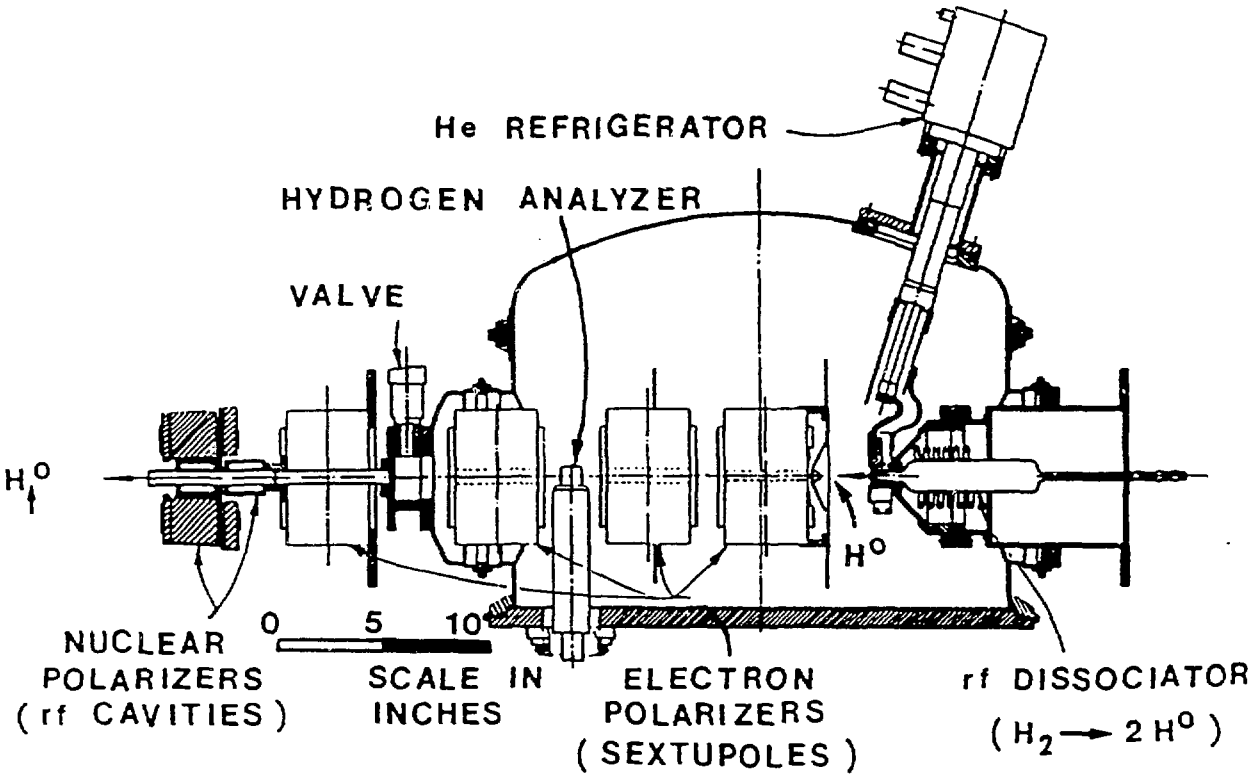

Fig. 1 Atomic-beam stage of the polarized-ion source.

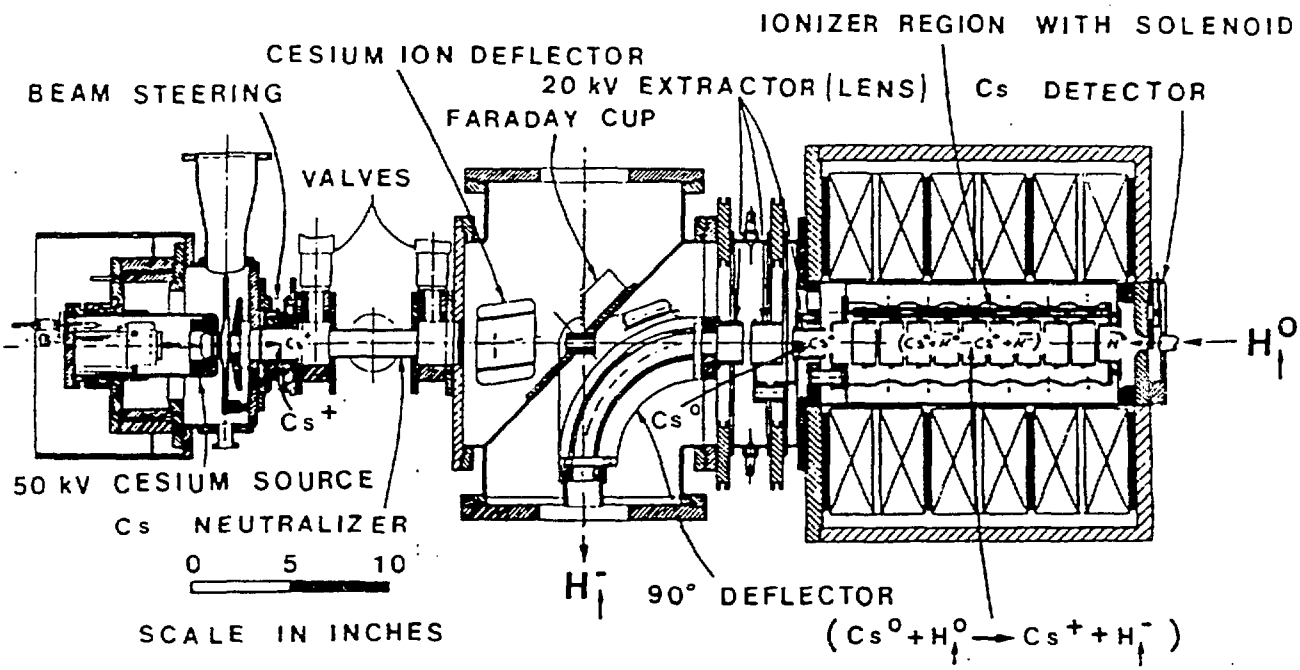

Fig. 2 Cesium source, extractor, and ionization region of the polarized-ion source.

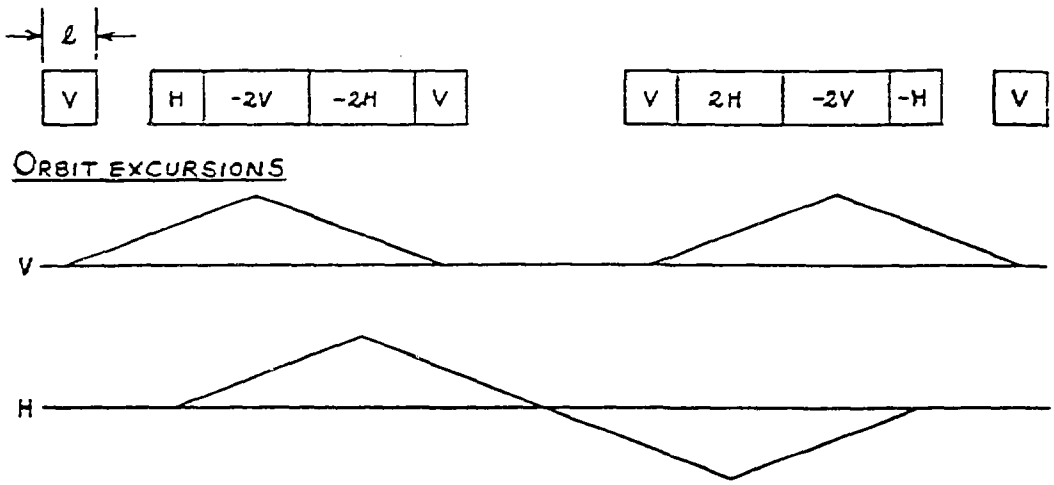

	Conventional dipole	Superconducting dipole
Field B	1.83 T	5.48 T
Unit length ℓ	0.75 m	0.25 m
Total length 19ℓ	14.25 m	4.75 m
Orbit excursion $\Delta x=\Delta z$	1.15 m/$\beta\gamma$	0.38 m/$\beta\gamma$

Fig. 3 Type 1 (longitudinal) Siberian snake precesses the spin 180° about the longitudinal axis. For the proton each unit has $B\ell$ = 1.37 Tm and precesses the spin 45°. H and V denote horizontal and vertical orbital deflections.

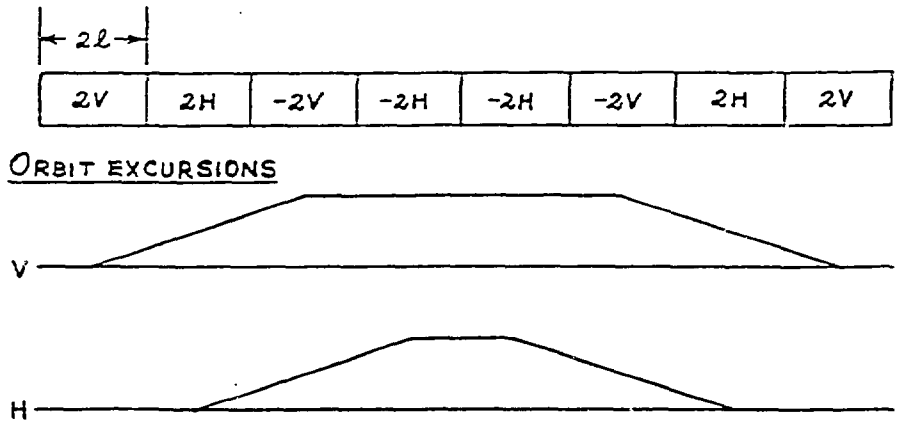

	Conventional dipole	Superconducting dipole
Field B	1.83 T	5.48 T
Unit length ℓ	0.75 m	0.25 m
Total length 16ℓ	12 m	4 m
Orbit excursion $\Delta x=\Delta z$	2.63 m/$\beta\gamma$	0.88 m/$\beta\gamma$

Fig. 4 Type 2 (transverse) Siberian snake precesses the spin 180° about the transverse (x) axis. For the proton each unit has $B\ell$ = 1.37 Tm and precesses the spin 45°. H and V denote horizontal and vertical orbit deflections.

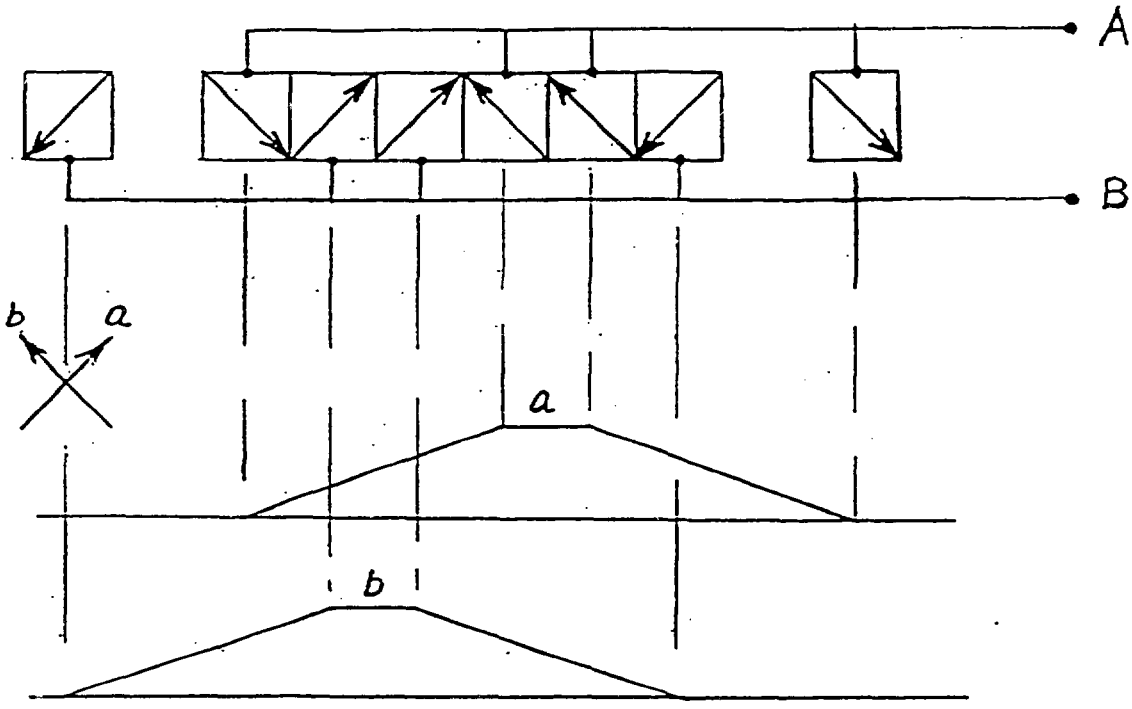

Parameters at $\delta = 90^{o}$

(A and B strings identical at $\delta = 90^{o}$)

Unit precession	45^{o}
Field B	5.48T
Unit length ℓ	0.25m
Total length, 10ℓ	2.5 m
Orbit excursion	$a = b = \frac{0.328m}{\beta\gamma}$

Fig. 5 Type 1 (longitudinal) variable precession snake ($\delta, \pi/2$) designed by Underwood. The snake has 8 skew (45^{o}-roll) dipoles powered in two strings A and B, and has a precession range of $\delta = 0^{o}$ to 90^{o}.

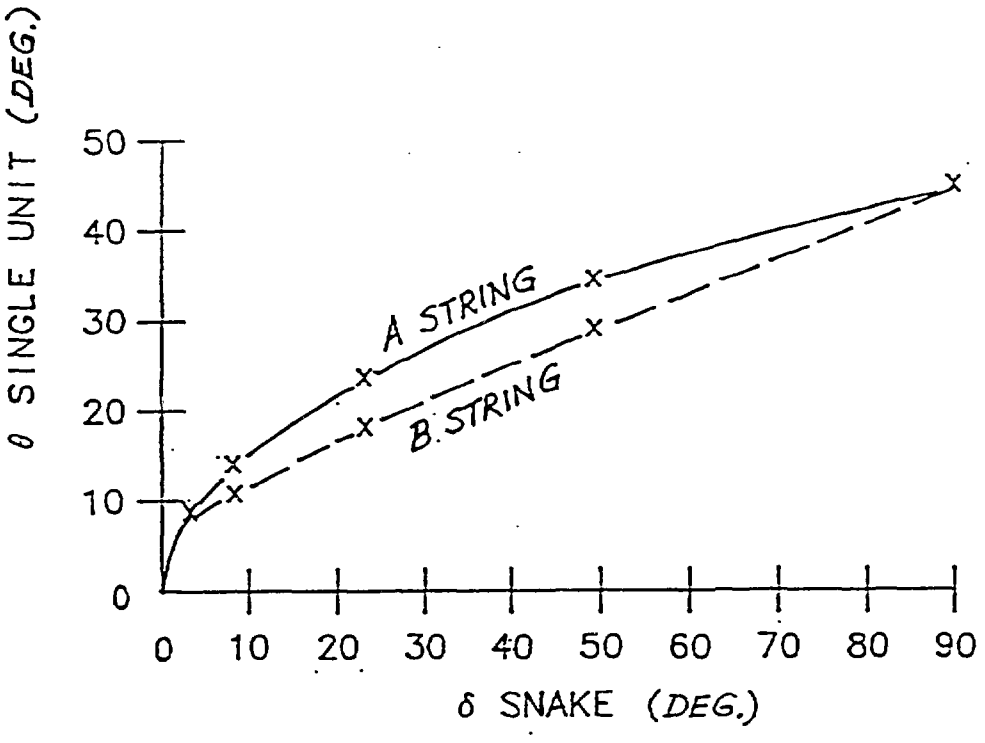

Fig. 6 Unit dipole precession angle θ in the A and B strings as functions of the snake precession angle δ for the Type 1 snake $(\delta,\pi/2)$ of Fig. 5. The function of the stronger string A is given approximately by $\theta^2 = (22.5^o)\delta$ over the range of $\delta = 0^o$ to 90^o.

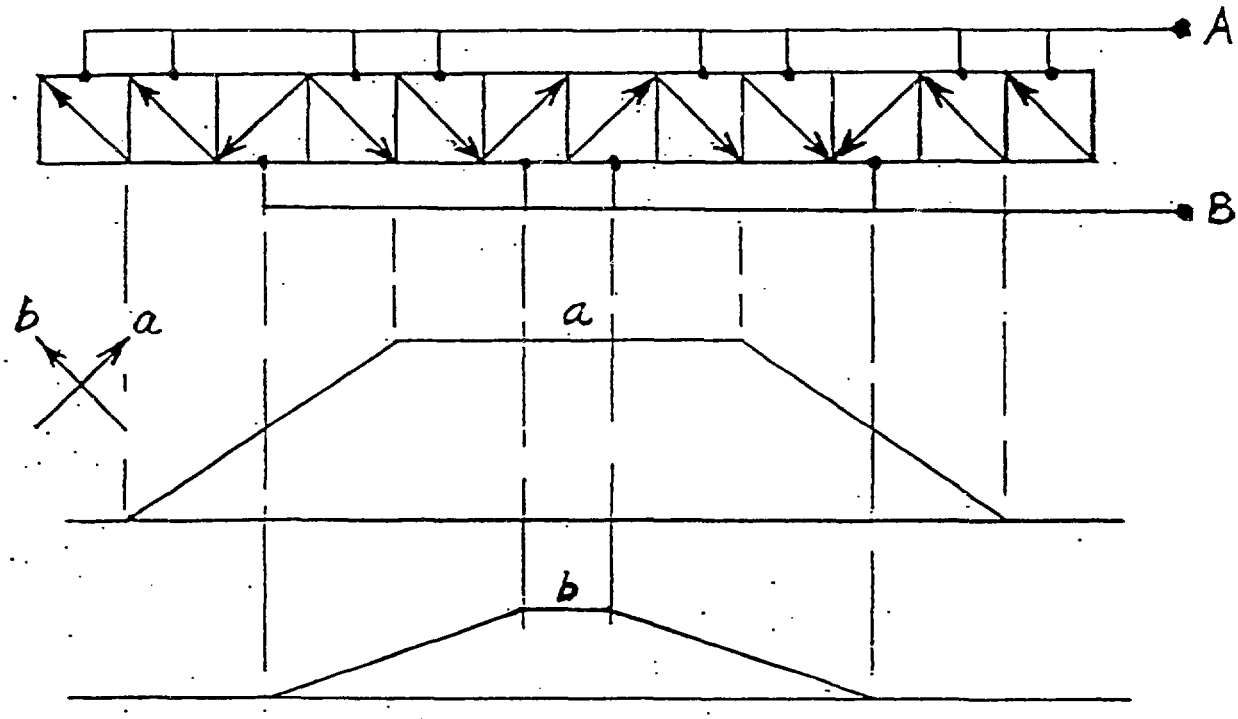

Parameters at $\delta = 90^{o}$

(A and B strings identical at $\delta = 90^{o}$)

Precession per dipole unit		45^{o}
Field B		5.48T
Unit length ℓ		0.25m
Total length 12ℓ		3m
Orbit excursion	$a = \frac{0.656\text{m}}{\beta\gamma}$	$b = \frac{0.328\text{m}}{\beta\gamma}$

Fig. 7 Type 2 (transverse) variable precession snake (δ,0) designed by D. Underwood. The snake has 12 skew (45^{o}-roll) dipoles powered in two strings A and B, and has a precession range of $\delta = 0^{o}$ to 180^{o}.

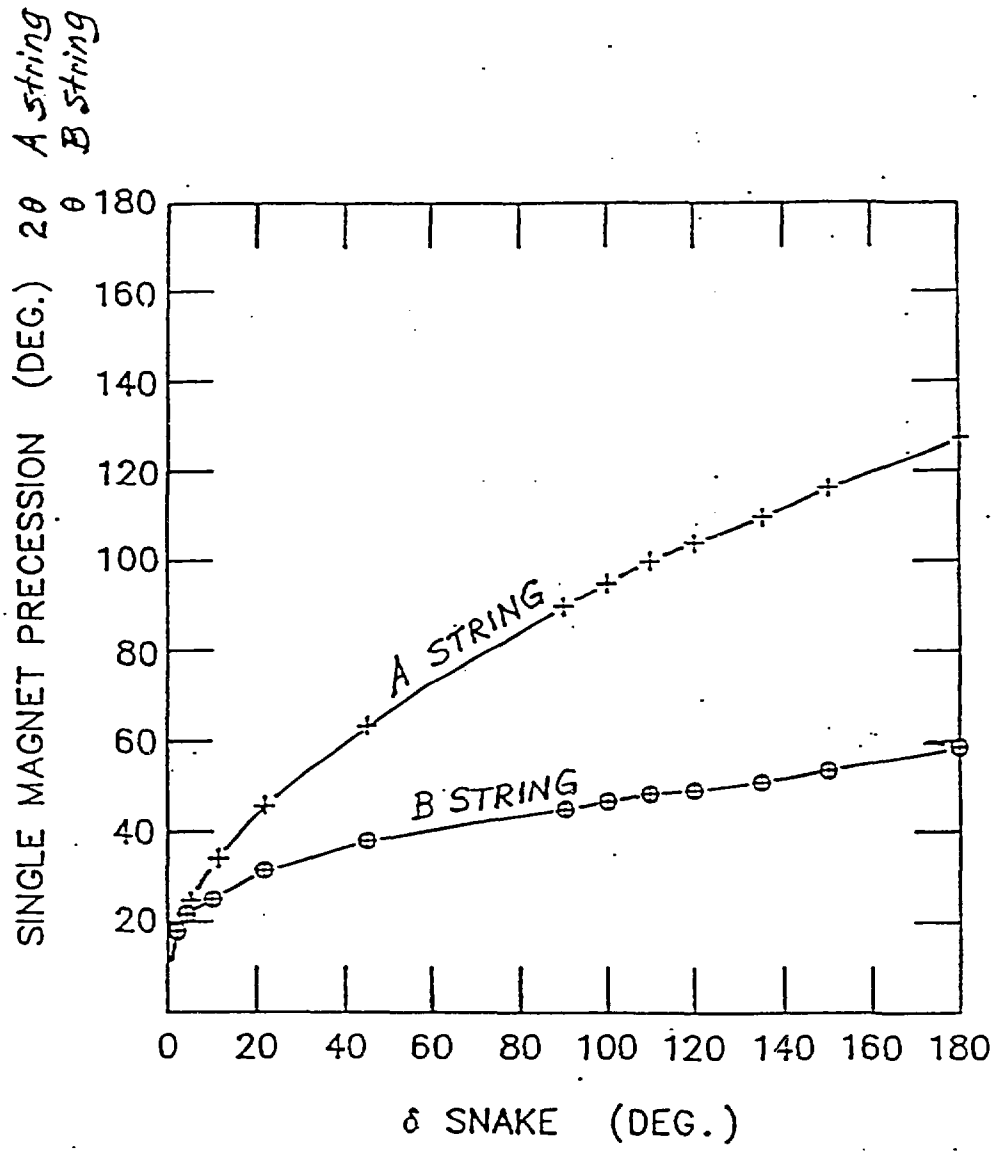

Fig. 8 Unit dipole precession angle θ in the A and B strings as functions of the snake precession angle δ for the Type 2 snake (δ,0) of Fig. 7. The function of the stronger string A is given approximately by $\theta^2 = (22.5^o)\delta$ over the range of $\delta = 0^o$ to 180^o.

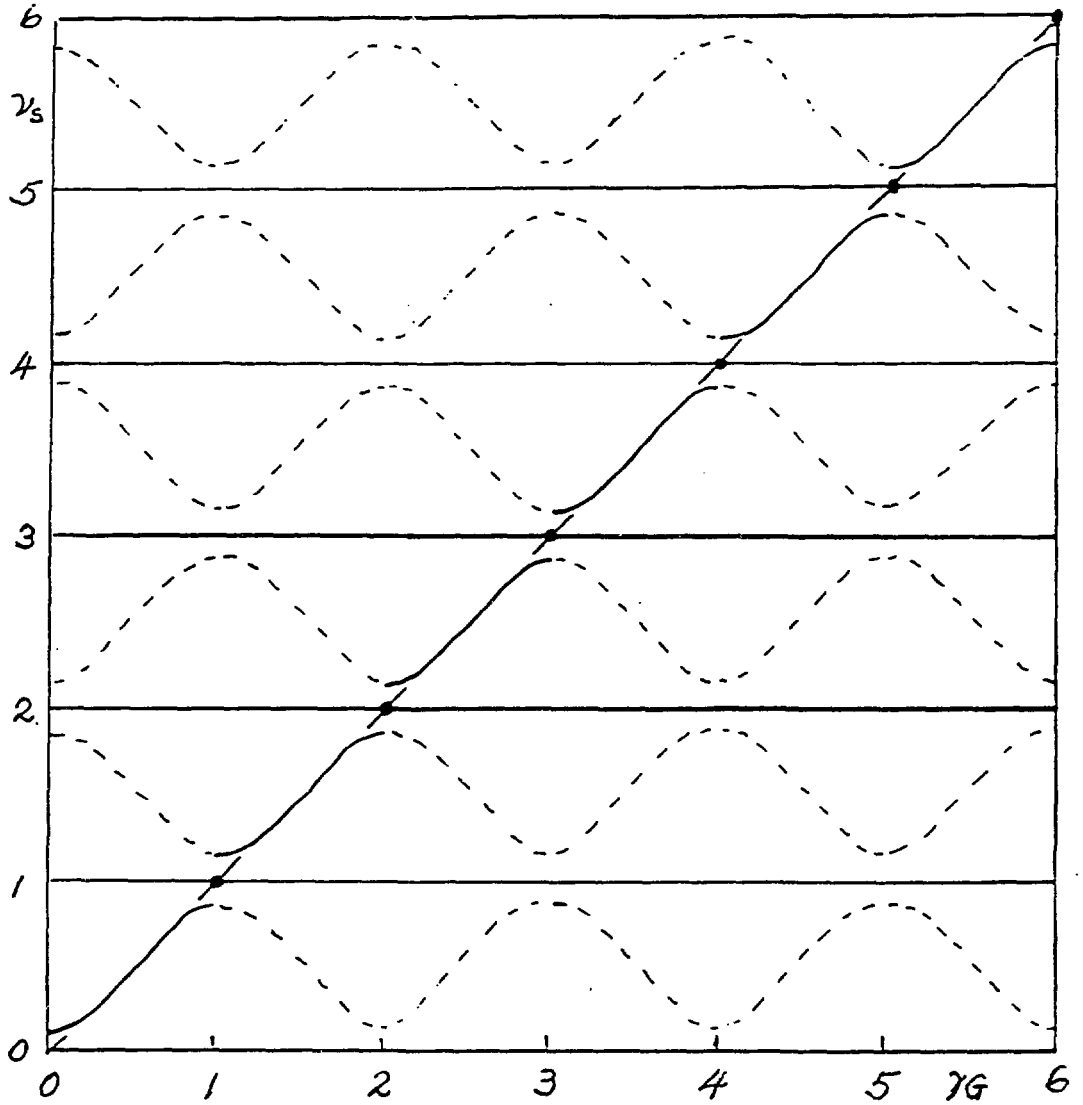

Fig. 9 Spin tune ν_s plotted against γG for a ring with a $\delta = 45^0$ partial snake showing the bands of available ν_s values and the exclusion of values near integers.

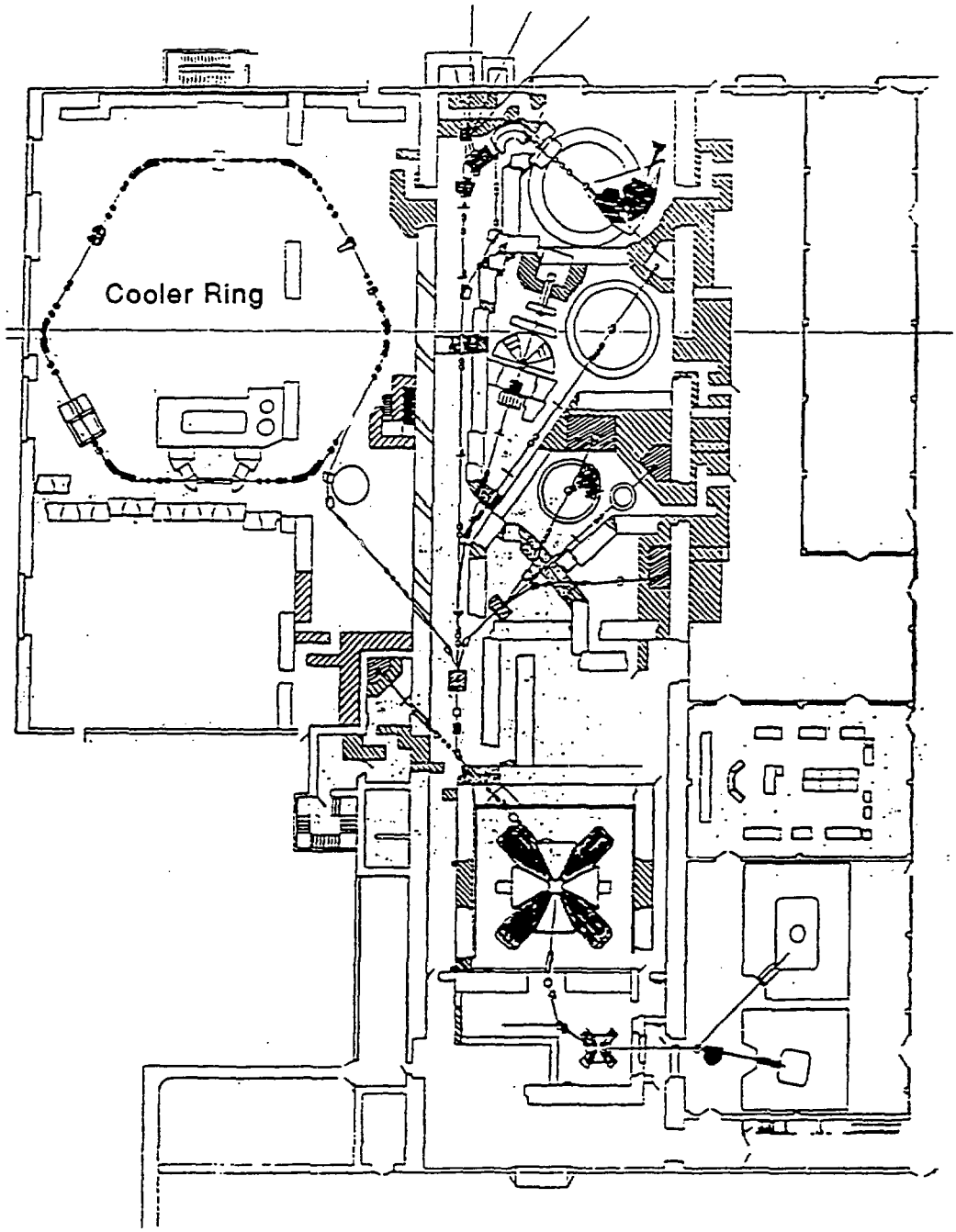

Fig. 10 Layout of the Indiana University Cyclotron Facility showing the Injector Cyclotrons, the Cooler Ring and other experimental areas and equipment.

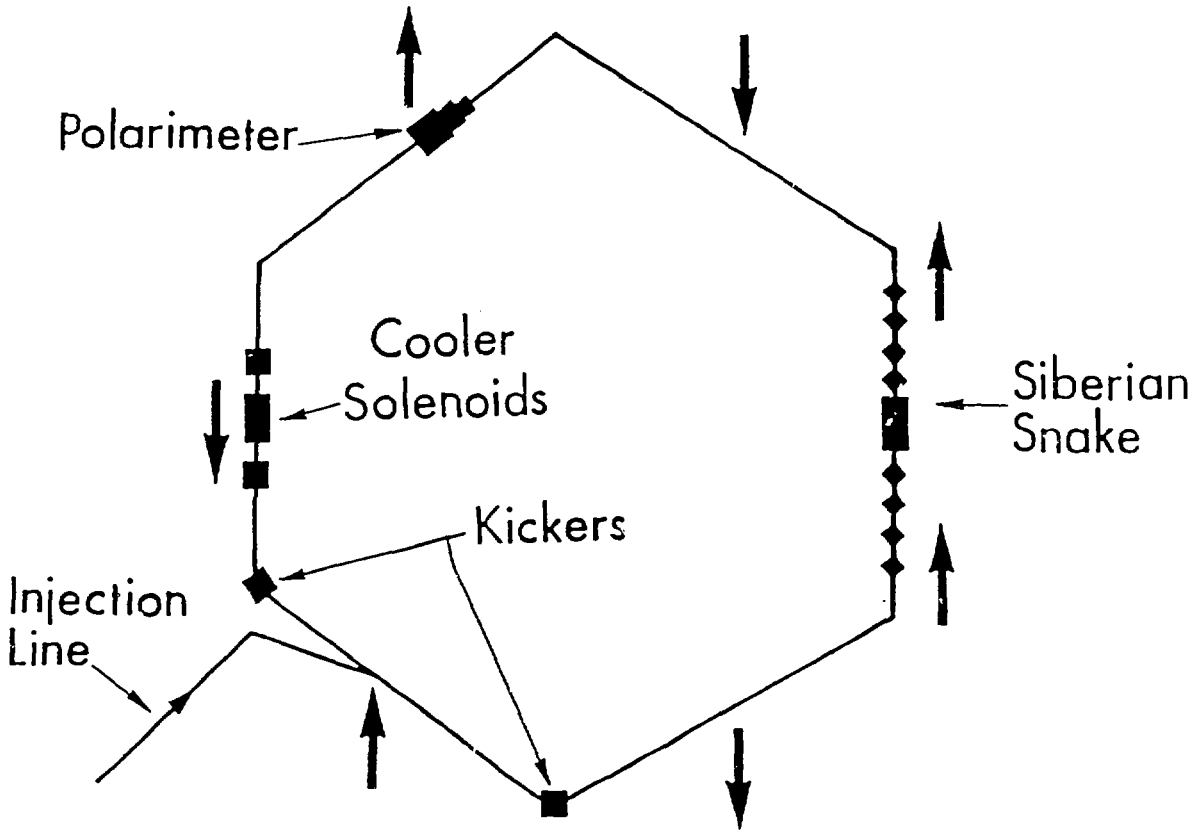

Fig. 11 Diagram of the IUCF Cooler Ring with the solenoid Type 1 Siberian snake installed.

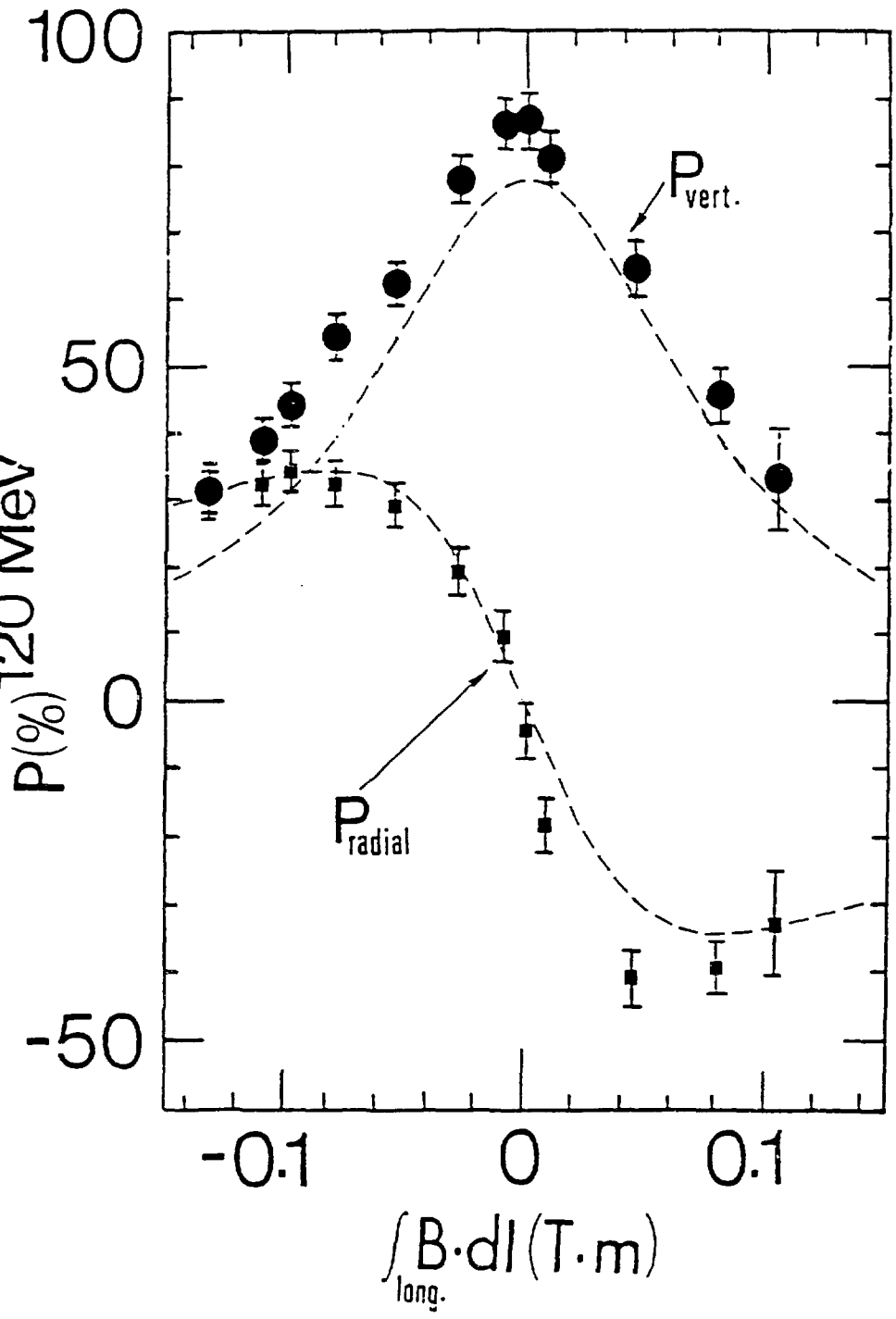

Fig. 12 The vertical and radial components of the beam polarization at 120 MeV are plotted against the longitudinal magnetic field integral in the Cooler solenoids with the Snake off and the injection of vertically polarized protons.

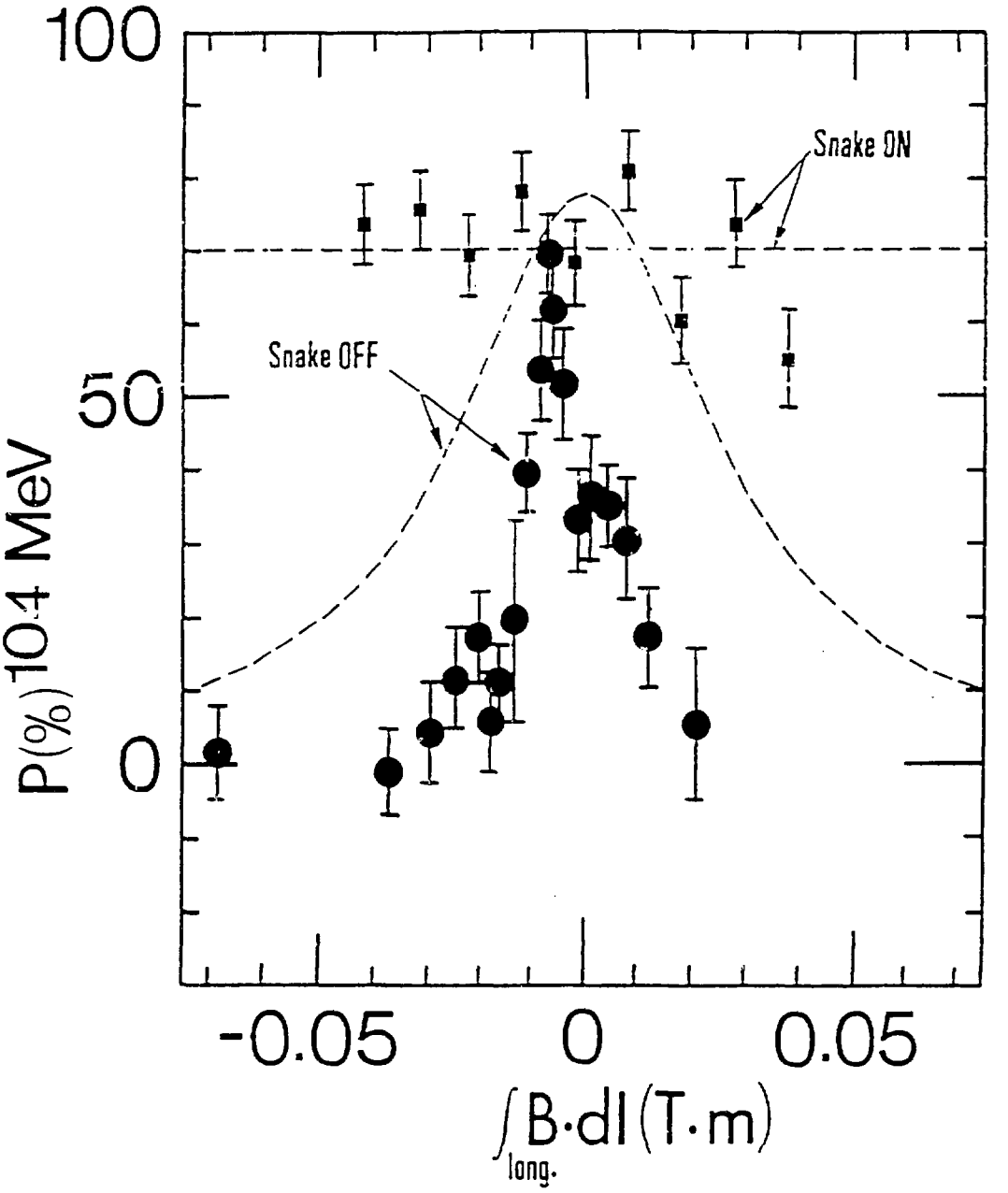

Fig. 13 The beam polarization in each stable polarization direction at 104 MeV is plotted against the longitudinal magnetic field integral in the Cooler solenoids. The large circles are the vertical polarization with the Snake off and the injection of vertically polarized protons. The small squares are the radial polarization with the Snake on and the injection of horizontally polarized protons.

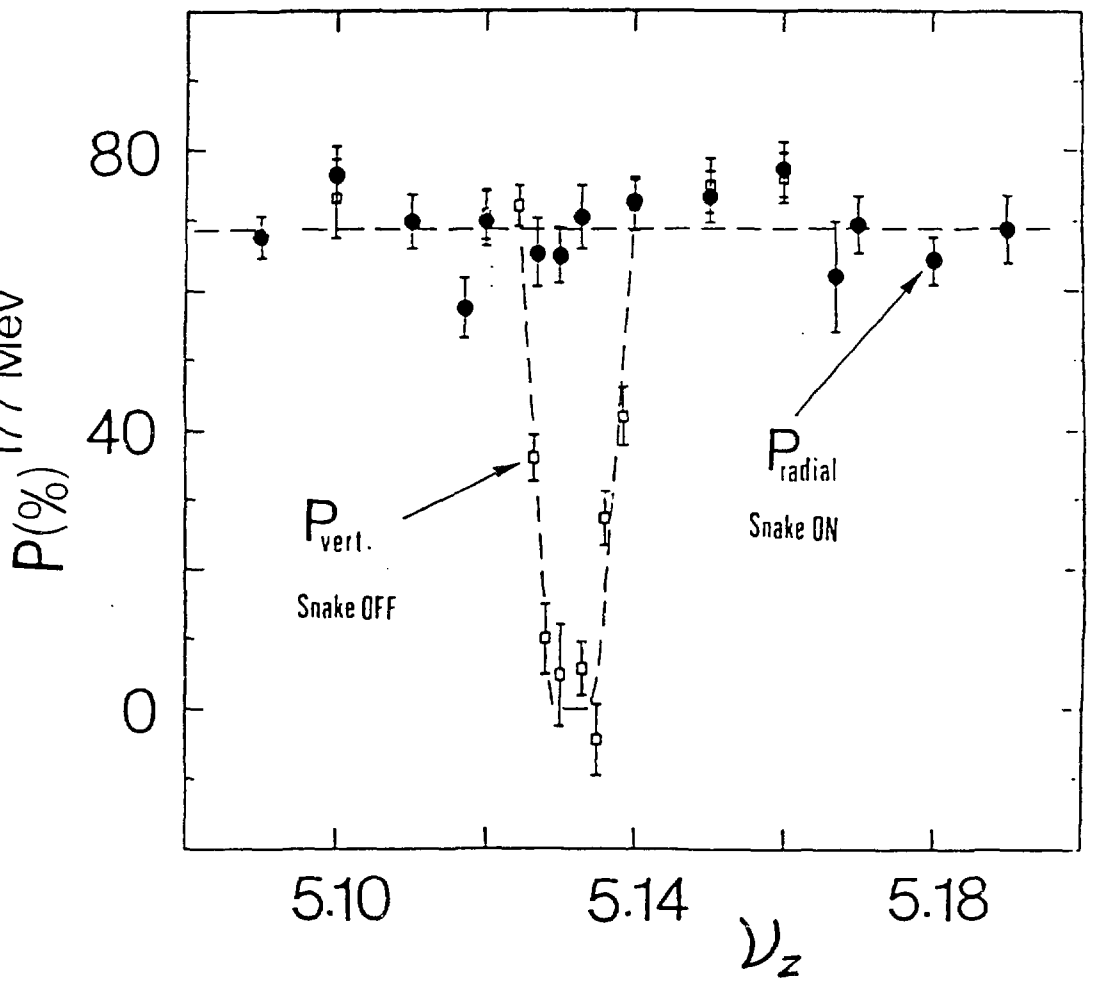

Fig. 14 The beam polarization in each stable spin direction at 177 MeV is plotted against the vertical betatron tune ν_z. The large circles are the radial polarization with the Snake on and the injection of horizontally polarized protons. The small squares are the vertical polarization with the Snake off and the injection of vertically polarized protons.